

FOUNDATIONS OF LARGE LANGUAGE MODEL COMPRESSION—PART 1: WEIGHT QUANTIZATION

Sean I. Young

siyoung@csail.mit.edu

ABSTRACT

In recent years, compression of large language models (LLMs) has emerged as an important problem to allow language model deployment on resource-constrained devices, reduce computational costs, and mitigate the environmental footprint of large-scale AI infrastructure. In this paper, we present the foundations of LLM quantization from a convex optimization perspective and propose a quantization method that builds on these foundations and outperforms previous methods. Our quantization framework, CVXQ, scales to models containing hundreds of billions of weight parameters and provides users with the flexibility to compress models to any specified model size, post-training. A reference implementation of CVXQ can be obtained from <https://github.com/seannz/cvxq>.

1 INTRODUCTION

Large language Models (LLMs) have become a universal framework for solving a vast number of problems in natural language processing, from text translation and summarization to conversational AI and automatic generation of radiologist’s reports. While LLMs outperform traditional methods in language-related tasks, they often involve tens or hundreds of billions of weight parameters, and this renders their deployment onto devices with limited resources challenging—model weights and activations no longer fit in the device memory, necessitating those activations be saved to and loaded from off-chip memory frequently during the course of inference. Not only does this greatly hinder the usability of LLMs particularly in time-sensitive tasks but it also exacerbates the environmental footprint of large-scale AI infrastructure required by LLMs.

One way to reduce the computational and storage requirements of large models is by compressing (that is, simplifying) the representation of the models post-training. Generally speaking, this can be achieved via weight pruning, quantization of activations and weights, or PCA-type dimensionality reduction of weight matrices. Out of these, quantization of weights and activation has proven to be particularly useful for compressing models to very low bit depths or arbitrary user-specified model sizes [1–15]. Using state-of-the-art quantization techniques, it is now possible to compress 10–100 billion-parameter LLMs to four bits per weight on average with negligible loss of model accuracy [8, 12], facilitating LLM inference on a single consumer-grade GPU.

Despite numerous advances, LLM quantization unfortunately remains far from solved. Not only do current weight quantization methods frequently lead to severely reduced model accuracy at low bit-depths, but most of these techniques have been developed specifically for weight quantization and are too complex to apply to activations during inference. Given the symmetry between weights and hidden states in matrix multiplications, achieving fast and accurate quantization of both weights and activations is crucial for enhancing computational efficiency and prediction accuracy, as well as for informing hardware design. This work aims to address these technological gaps in the current model compression literature and advance accurate and efficient compression methods for LLMs.

In this paper—the first of a three-part series—we lay the foundations of LLM compression within the classical framework of convex optimization. We begin with the problem of weight quantization and ask: How should the weights of a model be quantized to maximize prediction accuracy given a target model size in bits? We then propose a stochastic gradient ascent-type algorithm to solve this

problem exactly and efficiently post-training—in minutes for billion-parameter models and in a few hours for 10–100-billion-parameter models. Compared with the recent OPTQ family of approaches [7–9], our algorithm spends virtually zero time on actual weight quantization once the optimal bit depths have been determined. This renders our framework suitable also for quantizing intermediate activations, where the quantization procedure must not introduce significant delays to the inference pipeline. Our sequel—Part 2: Activation Quantization—discusses this in detail.

2 PREVIOUS WORK

Model quantization can be traced back to the early work of Vanhoucke et al. [16], who demonstrated that 8-bit integer arithmetic can be used for network training and inference without significant loss of accuracy. More generally, quantization-aware training (QAT) [17–22] integrates the quantization process into the training phase by allowing the model to adapt to the reduced precision in weights [17–20] and activations [21, 22] by determining the optimal bit depth [19, 22] and step size [20] by back-propagation, with some techniques even allowing the gradients to flow through quantization operators. One shortcoming of QAT methods is that model training needs to be repeated for different quantized model sizes and accuracy, rendering them less ideal for the quantization of large models requiring substantial compute and time for training.

More recently proposed quantization techniques for language and vision models focus primarily on rapid deployment of already trained models without retraining [4–15]. These approaches quantize model weights to 3–4 or 8 bits for integer-arithmetic-only inference [18] while separately handling outlier channels [23] or using mixed bit depth quantization [22, 11] to improve the quantized model accuracy. Loss-aware quantization techniques [24–26] seek to minimize accuracy loss in quantized models by calibrating quantization and biases on calibration data. Data-free quantization methods [27–30] attempt to remove the need for real calibration data by calibrating the distribution of weights instead [27] or using synthetic data in place of real calibration data [29].

For LLM compression in particular, a variant of the Optimum Brain Surgeon (OBS) algorithm [31] known as GPTQ [8] has been proposed for quantization of 1–100 billion parameter models. More recent extensions to GPTQ [9, 15] additionally incorporate handling of sensitive weights by scaling or simply by retaining the original weight values, with other approaches [6, 12] also independently incorporating similar ideas. Later, we will see that our convex optimization formulation provides a disciplined approach to incorporating channel sensitivity and scales into the quantization task.

3 QUANTIZATION FRAMEWORK

Here, we use the task of next-token prediction in language modeling as a running example. For our purposes, the end-to-end mapping of input token embeddings to predicted next-token embeddings defined by a pretrained language model f can be expressed in the most general form as

$$\mathbf{Z} = f(\mathbf{X}) = f(\mathbf{X}, \Theta_1, \Theta_2, \dots, \Theta_N) = f(\mathbf{X}, \Theta_1, \Theta_2, \dots, \Theta_N, \mathbf{B}_1, \mathbf{B}_2, \dots, \mathbf{B}_N) \quad (1)$$

in which $\mathbf{X} \in \mathbb{R}^{H \times E}$ denotes a sequence of L tokens, each of which resides in some E -dimensional embedding space, and $\mathbf{Z} \in \mathbb{R}^{L \times E}$, embeddings of L predicted next tokens. The m th block of weight matrices $\Theta_{mM+1}, \dots, \Theta_{(m+1)M}$ and bias vectors $\mathbf{B}_{mM+1}, \dots, \mathbf{B}_{(m+1)M}$ jointly parameterize the m th transformer block, which refines the embeddings produced by the $(m-1)$ th transformer block. In practice, LLM frameworks used in language modeling also require an embedder $\Theta_0 \in \mathbb{R}^{E \times V}$ and a prediction head $\Theta_{N+1} \in \mathbb{R}^{V \times E}$ for transforming between tokens and embeddings, but for now, we focus on the compression of transformer block weights as typically done in previous work [8, 9, 12].

To get a sense of the number of weight matrices and their sizes in a typical language model, the 13 billion-parameter model in the OPT family (OPT-13B) contains $N = 240$ weight matrices in blocks of $M = 6$, with each block comprising $12E^2$ weights in an embedding dimension of $E = 5120$. The embedder and prediction head are parameterized by a shared matrix containing VE weights, where the vocabulary size $V = 50272$. Note that each transformer block also contains $9E$ bias parameters but due to their relative scarcity, bias parameters can be communicated losslessly and still have little to no impact on the overall compression performance.

Notionally, the elements of a weight matrix Θ are continuously valued so they require quantization for efficient communication or storage. Compared with vector quantization and lattice quantization

Algorithm 1. CVXQ: Convex Optimization for Weight Quantization

```

1 Input:  $f(\cdot, \Theta_1, \dots, \Theta_N)$  (model),  $\{\mathbf{X}\}$  (calibration set),  $R$  (target bit rate),  $B_{\max}$  (max bit depth)
2 Output:  $\Theta_1^q, \dots, \Theta_N^q$  (quantized weights),  $B_1^*, \dots, B_N^*$  (bit depths),  $S_1, \dots, S_N$  (weight scales)
3 Initialize:  $\mathbf{U} \leftarrow \text{pca\_basis}(\{\mathbf{X}\}) \in \mathbb{R}^{E \times E}$ ,  $\mathbf{S} \leftarrow \text{sub\_sample}(\mathbf{I}_{L \times L}) \in \mathbb{R}^{L \times L}$ 
4    $B_n \leftarrow \infty$ ,  $V \leftarrow 10^{-6}$ ,  $G_n^2 \leftarrow 0$ ,  $S_n \leftarrow \text{std}(\Theta_n)$ ,  $\Theta_n^q \leftarrow \Theta_n$ ,  $B_n^q \leftarrow B_n$ ,  $\bar{\mathbf{X}}_n \leftarrow \mathbf{0}$  for  $n$  in  $1, \dots, N$ 
5 for iter in  $1, \dots, \text{max\_iter}$  do
6   for  $\mathbf{X}$  in minibatch do
7      $\mathbf{Z}, \mathbf{X}_1, \dots, \mathbf{X}_N \leftarrow f(\mathbf{X}, \Theta_1^q, \dots, \Theta_N^q, B_1^q, \dots, B_N^q)$ 
8      $\bar{\mathbf{X}}_n \leftarrow (1 - \alpha)\bar{\mathbf{X}}_n + (\alpha/L)\mathbf{1}^T \mathbf{X}_n$  for  $n$  in  $1, \dots, N$ 
9      $\Gamma_1, \dots, \Gamma_N \leftarrow \text{autograd}(\mathbf{S}^T \mathbf{Z} \mathbf{U}, \Theta_1^q, \dots, \Theta_N^q)$ 
10     $G_n^2 \leftarrow (1 - \alpha)G_n^2 + (\alpha/P_n) \text{trace}(\Gamma_n^T \Gamma_n)$  for  $n$  in  $1, \dots, N$ 
11  for _ in  $1, \dots, 10$  do
12     $B_n \leftarrow \text{clamp}(\frac{1}{2} \log_2(G_n^2 S_n^2 / V), 0, B_{\max})$  for  $n$  in  $1, \dots, N$ 
13     $V \leftarrow V + \beta(\text{sum}(P_n B_n) - (\text{sum}(P_n))R)$ 
14   $\Theta_n^q \leftarrow \text{compand\_quantize}(\Theta_n, B_n, S_n)$ ,  $B_n^q \leftarrow B_n + (\Theta_n^q - \Theta_n)\bar{\mathbf{X}}_n$  for  $n$  in  $1, \dots, N$ 

```

approaches [32], scalar quantization enables arithmetic operations to be performed on quantization indices directly, eliminating the need for a separate dequantization process. The mid-rise uniform scalar quantization of a weight θ at a bit-depth of B bits and step size D gives us the reconstruction

$$\theta^q(B, D) = D(\text{clip}(\text{floor}(D^{-1}\theta), -2^{B-1}, 2^{B-1} - 1) + 2^{-1}), \quad B = 0, 1, 2, \dots \quad (2)$$

and $\theta^q(B, D) = \theta$ if $B = \infty$ for notational convenience. The problem of compressing the model f now amounts to determining the optimal bit depth B and the associated quantization step size D for each weight. However, it would be impractical to determine a separate (B, D) for each weight θ in the model since the cost of signaling the choice of (B, D) for each one would far outweigh the saving derived from quantization. Typically, a single (B, D) pair is used to quantize a group of weights (an entire matrix or rows or columns thereof) in which case the cost of signaling (B, D) can be borne by a group of quantized weight parameters as a negligible per-weight overhead.

3.1 BIT DEPTH ASSIGNMENT

Suppose we want to compress f by quantizing each matrix Θ_n containing P_n elements according to its own bit depth B_n and step size $D_n^*(B_n)$. How should B_n be decided? Roughly speaking, weights that are more sensitive to output distortion should be allotted more bits to “balance the scales” while keeping the total number of bits under a given model bit budget. One can formalize this notion by expressing the quantization task at hand as the optimization problem

$$\text{minimize } d(B_1, \dots, B_N) = \mathbb{E}_{\mathbf{X}} \|f(\mathbf{X}, \Theta_1^q(B_1, D_1^*(B_1)), \dots, \Theta_N^q(B_N, D_N^*(B_N))) - f(\mathbf{X})\|_F^2 \quad (3)$$

$$\text{subject to } r(B_1, \dots, B_N) = \sum_{n=1}^N P_n B_n - (\sum_{n=1}^N P_n) R = 0$$

in which R denotes a user-specified average model bit depth (bit rate). This problem is reminiscent of optimal resource allocation, where the objective is to maximize some utility (or minimize output distortion in our case) by optimally spending down a given budget (the total number of bits). In this section and next, we provide insights into problem (3) and our proposed approach; see Algorithm 1.

To apply the machinery of numerical optimization to (3), we will relax the discrete constraint on the bit depths B_1, \dots, B_N while solving the problem and round the solution B_1^*, \dots, B_N^* to the nearest integers after they have been obtained. Let us write the Lagrangian of (3) as $\mathcal{L}(B_1, \dots, B_N, V) = d(B_1, \dots, B_N) + Vr(B_1, \dots, B_N)$, where V is a dual variable associated with the equality constraint of (3). Differentiating \mathcal{L} with respect to B_1, \dots, B_N, V gives us the first-order optimality conditions

$$\frac{1}{P_1} \frac{\partial d(B_1^*, B_2^*, \dots, B_N^*)}{\partial B_1} = \dots = \frac{1}{P_N} \frac{\partial d(B_1^*, B_2^*, \dots, B_N^*)}{\partial B_N} = -V, \quad r(B_1^*, \dots, B_N^*) = 0 \quad (4)$$

so problem (3) can be solved by alternately updating the bit depths B_1, \dots, B_N (primal variables) and the trade-off V (dual variable) until all optimality conditions are met. In words, the optimality conditions are reached once the marginal decrease in the output distortion from an infinitesimal bit is equal across layers at $-V$ and once we have assigned exactly R bits per weight on average.

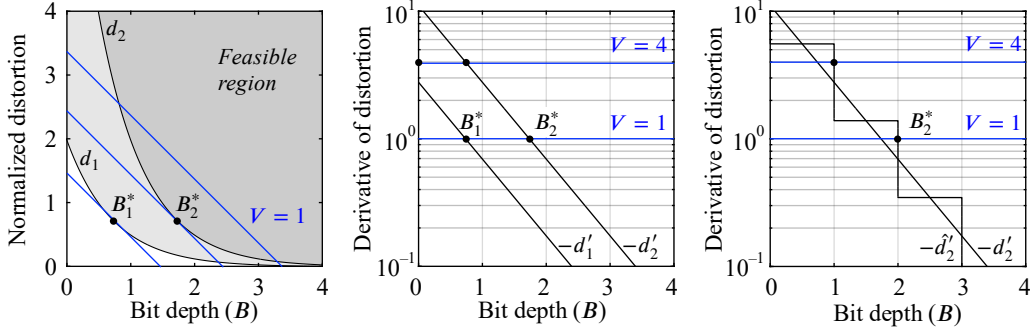


Figure 1: Optimal bit depths. Consider two weight matrices whose distortion functions are given by d_1 and d_2 , where $d_n(B_n) = G_n^2 S_n^2 2^{-2B_n}$. For any given value of the dual variable V , optimal bit depths B_1^* and B_2^* are found where the derivative of d_1 and d_2 is $-V$, respectively (left). These points correspond to the intersections between V and $-d'_n = (2 \ln 2) d'_n$ (center). Integerized bit depths occur on the rounded curves $-\hat{d}'_n$ (right).

Since the quantization function (2) is constant almost everywhere, a naive computation of the partial derivatives of d with respect to B_1, \dots, B_N using the chain rule of differentiation does not provide a useful direction for descent. A well-known result from rate–distortion theory [33] is that for any random variable of finite variance, quantization error decreases by half with every additional bit at a sufficiently high bit depth. More specifically to our problem, we can write (Appendix A)

$$-\frac{1}{2 \ln 2} \frac{\partial d(B_1, \dots, B_N)}{\partial B_n} \approx \mathbb{E}_{\mathbf{X}} \left\| \frac{\partial f(\Theta_1^q(B_1), \dots, \Theta_N^q(B_N))}{\partial \Theta_n} \cdot \Delta_n^q(B_n) \right\|_F^2 \approx P_n H_n \underbrace{G_n^2 S_n^2 2^{-2B_n}}_{= d_n(B_n)} \quad (5)$$

in which $\Theta_n^q(B_n) = \Theta_n^q(B_n, D_n^*(B_n))$ for brevity, G_n^2 and S_n^2 represent the variances of the elements of $\partial_{\Theta_n} f(\mathbf{X}, \Theta_1, \dots, \Theta_N)$, and of Θ_n , respectively, and H_n is a quantization coefficient that depends on the distribution of weights, with $H_n = 1.42$ for Gaussian, 0.72 for Laplace, etc. [33]. Assuming that weights are distributed similarly across layers with $H_1 = \dots = H_N$, factors H_n (along with the global factor $-\frac{1}{2 \ln 2}$) can be removed the above expression without affecting the solution of (3).

Coupled with the above closed-form expression for the partial derivatives, optimality conditions (4) lend themselves naturally to dual ascent-type methods for solving problem (3). The idea behind dual ascent [34] is to alternately update the primal variables B_1, \dots, B_N , and the dual V , holding one set fixed while updating the other. After initializing $B_1 = B_2 = \dots = B_N = \infty$, and V to a small positive number, the bit depths (primal) and trade-off (dual) are updated at every iteration as

$$B_n \leftarrow \text{clamp} \left(\frac{1}{2} \log_2 \left(\frac{G_n^2 S_n^2}{V} \right), 0, B_{\max} \right) \quad \text{for } n = 1, \dots, N \quad (6)$$

$$V \leftarrow V + \alpha \left(\sum_{n=1}^N P_n B_n - \left(\sum_{n=1}^N P_n \right) R \right)$$

in which α denotes a step size for dual update. With G_n^2 and S_n^2 fixed, dual ascent steps (6) always converge within a few iterations ($\text{tol} \approx 10^{-6}$ bit) for a suitably chosen step size. Figure 1 illustrates the conditions for optimal bit depths at any given value of the dual variable. Upon convergence, B_n is rounded to an integer and used to quantize the weight matrix Θ_n (Algorithm 1, ln 11–14).

For the primal update in (6), one key question is how the gradient variance G_n^2 —the variance of the elements of $\partial_{\Theta_n} f(\mathbf{X}, \Theta_1, \dots, \Theta_N)$ —should be accumulated. Accumulating these variances across the entire calibration set at every iteration is prohibitively expensive given the dimensionality of the output $f(\mathbf{X}) \in \mathbb{R}^{L \times E}$ and the cost of back-propagating each of its elements through f . To overcome this difficulty, we can perform PCA on $f(\mathbf{X})$ along the embedding dimension (of E) and sub-sample along the token dimension (of T), and accumulate variances by back-propagating only a minibatch of calibration examples every few iterations:

$$G_n^2 \leftarrow (1 - \beta) G_n^2 + \beta \mathbb{E}_{\mathbf{X} \sim \text{batch}} \left\| \frac{\partial \mathbf{S}^T f(\Theta_1^q(B_1), \dots, \Theta_N^q(B_N)) \mathbf{U}}{\partial \Theta_n} \right\|_F^2 \quad \text{for } n = 1, \dots, N \quad (7)$$

in which β denotes the learning rate, and \mathbf{S}^T and \mathbf{U} represent the PCA projection and sub-sampling

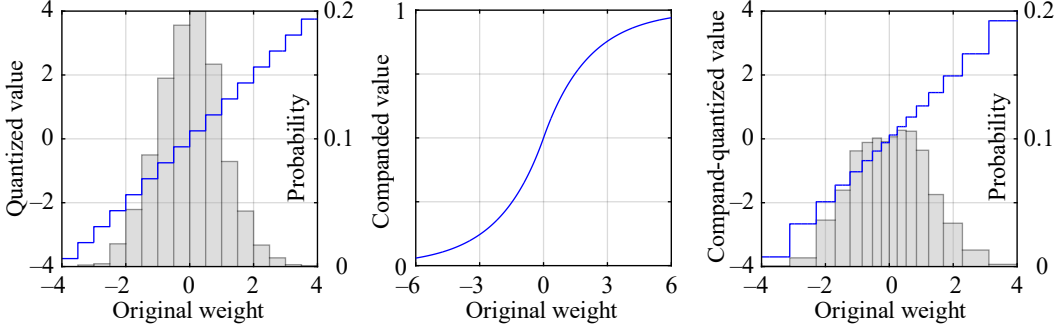


Figure 2: Companding quantization. Illustrated for a 4-bit quantizer (16 bins) on Gaussian weights with a mean of zero and a variance of one. Uniform quantization across the entire range of weight values (left) leads to unduly large quantization bins (hence errors) for more probable values. Companding the weights to the range (0,1) prior to uniform quantization (middle) reduces quantization errors for more probable weights (right).

operators, respectively. In practice, we further accelerate variance accumulation by cycling through PCA coefficients and back-propagating only one coefficient per sample in every batch.

3.2 STEP SIZES AND BIASES

Suppose now the weight matrices $\Theta_1, \dots, \Theta_N$ are to be assigned bit depths B_1, \dots, B_N (which are not necessarily optimal.) Our next question is: How should the quantization step size D_n be decided given bit depth B_n ? In the round-to-nearest scheme (RTN, Figure 2, left), D_n is always chosen such that the quantizer’s 2^{B_n} steps just cover the entire range of weight values, and this step size halves as B_n is increased by one. These criteria optimize step sizes when weights are distributed uniformly across a range and the objective is to minimize distortion in quantized weights. However, different considerations apply if our objective is to minimize distortion in the final embeddings as in (1).

In LLMs, the elements of a weight matrix typically exhibit a heavy-tailed distribution [23], which renders partitioning the entire weight range into 2^{B_n} equal steps sub-optimal especially at lower bit depths [33, 35]. One alternative to computationally expensive Lloyd–Max quantization [36, 37] is companded quantization [38], where weights are uniformly quantized in some sigmoid domain; see Figure 2, center and right). Since the output embeddings are Laplace distributed, one good choice of companding function for a weight matrix Θ_n with zero mean and variance S^2 is given by [33]:

$$\theta^c(S) = \frac{1 + \operatorname{sgn}(\theta - \mu)}{2} \exp\left(-\frac{\sqrt{2} \operatorname{abs}(\theta - \mu)}{3S}\right) \in (0, 1), \quad \theta \in (-\infty, \infty), \quad (8)$$

that is, the normalized cubic root of the cumulative distribution function for a Laplace distribution of zero mean and variance S^2 . The companded weights θ^c can then be quantized using the round-to-nearest scheme in the range (0, 1). The quantization indices are now signaled along with the bit depth B and scale S for efficient dequantization via lookup tables—no numerical evaluation of the inverse companding function need be performed. In practice, S is treated as a tunable parameter and refined efficiently on a coarse 1D grid as a post-processing step once Algorithm 1 has completed.

Quantization invariably causes small deterministic differences to arise between the original (non-quantized) Θ and quantized Θ^q weights. While these errors are often modeled as zero-mean noise in theoretical analyses, they are seldom zero-mean in practice and can lead to systematically biased model output, which significantly reduces prediction accuracy. To compensate for these non-zero differences, we compute new bias vectors for the model as $\mathbf{B}_n^q \leftarrow \mathbf{B}_n + (\Theta_n^q - \Theta_n) \bar{\mathbf{X}}_n$ each time the matrix Θ_n is quantized. Here, $\bar{\mathbf{X}}_n$ is a vector of running means of the inputs to the n th layer, which is accumulated during the forward pass in a manner analogous to the accumulation of G_n^2 during the backward pass. The corrected biases \mathbf{B}_n^q are then used whenever the corresponding quantized weight matrices Θ_n^q are used during gradient variance accumulation and inference.

3.3 MATRIX PARTITIONING

Rather than quantize optimally at the granularity of a whole weight matrix, we can split each matrix

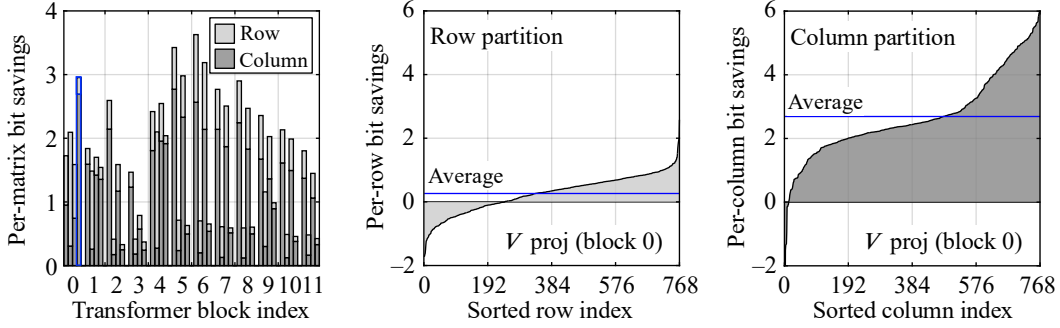


Figure 3: Bit savings from partitioning. Plotted for OPT-125m. Bit savings are derived by partitioning weight matrices into a collection of row or column matrices and assigning each sub-matrix its own bit depth. Savings differ across the (Q , K , V and O) projection matrices of the model’s 12 transformer blocks (left). Per-column (middle) and per-row (right) bit savings can sometimes dip below zero but are always positive on average.

into a collection of row or column matrices, assigning optimum bit depth and step size to each sub-matrix. In this case, the total number of matrices N in (3) can be reinterpreted as the total number of sub-matrices collected across all layers, with the quantities B_n , D_n and P_n , similarly interpreted as the bit-depth, step size and number of elements of the n th sub-matrix. Note that quantizing at the granularity of row or column sub-matrices does not noticeably increase the complexity of variance accumulation as the same squared gradients computed via back-propagation can be averaged per sub-matrix to produce the corresponding sub-matrix variances. Here, without loss of generality, we assume that each matrix is split into a collection of column matrices.

For a weight matrix Θ with gradient and weight variances G^2 and S^2 , whose per-column variances are G_1^2, \dots, G_N^2 and S_1^2, \dots, S_N^2 , respectively, the theoretical gain (average bit depth savings) from partitioning can be expressed as

$$\gamma_{\text{partition}} = \frac{1}{2} \left(\log_2(G^2 S^2) - \frac{1}{N} \sum_{n=1}^N \log_2(G_n^2 S_n^2) \right), \quad (9)$$

a non-negative quantity as a direct result of Jensen’s inequality. This quantity represents the bit-rate (average bit-depth) savings when the n th column is assigned $B_n = \frac{1}{2} \log_2(G_n^2 S_n^2) + B$ bits for some B , compared to assigning a uniform bit depth $B_n = \frac{1}{2} \log_2(G^2 S^2) + B$ bits across all columns under the assumption that the weights of its N columns are identically distributed. Figure 3 (left) plots the per-matrix bit-depth savings derived by partitioning the (Q , K , V and O) projection matrices of the OPT-125m model by rows or columns. The per-channel breakdown of the savings is also shown.

In addition to primary splitting of matrices into columns, we may want to further split each column into a fixed number of groups of weight elements given the benefits of row partitioning as well. To split the columns of a weight matrix $\Theta \in \mathbb{R}^{N \times N}$, one can simply cluster its rows into M similarly sized groups based on their row variances $G_1^2 S_1^2, \dots, G_N^2 S_N^2$. By applying the same clustering to all columns of a matrix, we can signal the cluster index for each row using $\lceil \log_2 M \rceil$ bits—a negligible per-weight overhead for a typical number of columns in a large matrix and the number of groups used in practice. We illustrate partitioning and subdivision in Figure 4. Table 2 (c) lists the accuracy of OPT models quantized using different numbers of row clusters, demonstrating that clustering in addition to partitioning is crucial for improved model accuracy.

4 QUANTIZATION EXPERIMENTS

To study the behavior of quantized LLMs on typical language tasks, we apply CVXQ (Algorithm 1) to Meta’s Open Pretrained Transformer (OPT) [39] and Llama 2 [40] families of language models (huggingface versions) on language modeling and mathematics problem solving tasks. We source calibration examples from the training split of the C4 dataset [41] for both tasks and validate on the test split of WikiText2 dataset [42] for language modeling and GSM8K [43] for math problems. A number of studies on hyperparameter tuning are also conducted using the C4 dataset.

Language Modeling. As our main set of experiments, we quantize Meta’s OPT and Llama 2 models to 3 and 4 bits, and measure the performance of the quantized models using perplexity, a stringent accuracy metric. We use row clusters with cluster size of 512 for OPT (768 for OPT-125M) and 256

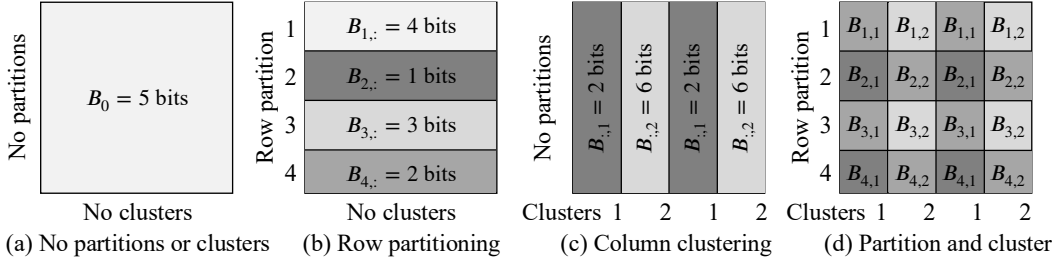


Figure 4: Partitioning and clustering. Illustrated for a 4×4 weight matrix. Rather than assign the same bit depth to all elements of a weight matrix (a), we can assign a separate bit depth to each row of weights (b), or to a cluster of columns (c), and even combine partitioning and clustering (d) to realize bit savings.

for Llama 2 models, accumulation batch size of 16, and 17 tokens from each sequence of tokens of length 2048, and optimize for 64 iterations maximum. Table 1 lists the perplexity of our quantized models (CVXQ) on the WikiText2 test set. While we perform quantized model selection based on the WikiText2 validation set, selecting the last quantized model produces similar test accuracy. For comparison, we include the perplexities of the same models quantized with round-to-nearest, GPTQ [8], OWQ [9], and AWQ [12] methods, using the code provided by the respective authors and with the default quantization and optimization hyperparameters; see Appendix B. Compared to the next best performing methods OWQ and AWQ, the proposed method provides a perplexity reduction of up to 4.55 for the 3-bit OPT-125M model although a minor perplexity gain (0.01–0.02) is observed for 3-bit OPT-66B and Llama 2 70B models. Note that AWQ in this comparison uses a group size of 128, incurring 2–4 times as many overhead bits as the proposed method, and OWQ by its nature operates at average per-weight bit depths that are 0.01–0.05 bits higher than the proposed method.

Effect of Hyperparameters. To study the effect of CVXQ hyperparameters on the accuracy of the quantized models, we quantize the OPT-1.3B and -13B models over a range of minibatch sizes and token counts (optimization hyperparameters) and cluster sizes (quantization hyperparameter), with each hyperparameter varied while keeping the others fixed at their optimized values. (The optimal hyperparameter values are batch size: 16, token count: 17, and cluster size: 512.) The perplexity of the quantized models is then measured on the C4 test data. Table 2 (a–b) demonstrates that CVXQ is largely insensitive to the values of optimization hyperparameters over a wide range. From Table 2 (c), we see that smaller cluster sizes generally improve the performance of the quantized models at lower average bit depths, but this also leads to higher overheads (discussed next). Figure 5 plots quantized model accuracy across optimization iterations when the baseline hyperparameter values are used, showing that less than 10 iterations are needed for quantization parameters (clustering and bit depth decisions) to converge.

Pruning Due to Quantization. CVXQ quantizes low-variance weights of weight matrices to zero and effects a form of weight pruning, which has been shown to improve generalization [31]. Table 3 (a) lists the percentages of zero-quantized weights in the OPT-1.3B and 13B models quantized to 3 and 4 bits per weight on average. In general, using a smaller cluster size increases the number of zero weights since this allows low-variance weights in a given column to be clustered together and quantized to zero. However, smaller clusters lead to higher overheads so that small improvements in generalization due to pruning come at the cost of signaling the overhead bits. Table 3 (b) lists the number of overhead bits (cluster indices and FP16 encodings of the location and scale parameters of each weight cluster) as a percentage of the total number of quantized weight bits.

Downstream Tasks (Grade School Math 8K). To study the impact of quantization on downstream tasks, we list in Table 4 (a) the accuracy of CVXQ-quantized Llama-2 models on the GSM8K (Grad School Math 8K) task [43], designed to evaluate the ability of language models to solve grade-level math word problems. Evaluation is performed in a 5-shot setup (flexible-extract filter). For a fairer evaluation, we match the group size of GPTQ and AWQ to our cluster size of 256. We observe that CVXQ produces relatively high scores especially for 3-bit quantized models whereas RTN leads to severely reduced scores despite having a similar perplexity as CVXQ on WikiText 2 (Table 1).

2.x-bit Llama-2. We study the accuracy of Llama 2 models quantized to 2.x bits using CVXQ and OWQ, both of which are capable of quantizing models to fractional average bit depths. To enable a more comprehensive study, we compare against OWQ with no grouping, as well as with group sizes of 128 and 256. We see from Table 4 (b) that CVXQ-quantized Llama-2 models are considerably

Table 1: WikiText2 perplexity. We quantize the Meta OPT and Llama 2 families of LLMs to 3–4 bits using the proposed quantization method, reporting the resulting perplexity of each quantized model on the WikiText2 dataset (test). For comparison, we also list the perplexities of models quantized using other approaches.

Perplexity (PPL)	WikiText2 (↓)	Meta OPT (Open Pretrained Transformer)							Meta Llama 2			
		125M	350M	1.3B	2.7B	6.7B	13B	30B	66B	7B	13B	70B
Full precision (FP16)		27.65	22.00	14.63	12.47	10.86	10.13	9.56	9.34	5.47	4.88	3.32
4 bits	RTN	37.28	25.94	48.17	16.92	12.10	11.32	10.98	111.36	5.73	4.98	3.46
	GPTQ [8]	32.05	23.87	15.47	12.83	11.14	10.29	9.57	9.34	5.69	4.98	3.42
	OWQ [9] (4.01 bits)	29.47	23.19	15.01	12.39	10.87	10.26	9.50	9.25	5.63	5.01	3.43
	AWQ [10]	29.11	–	14.95	12.74	10.93	10.22	9.59	9.39	5.60	4.97	3.41
	CVXQ (Ours)	27.90	22.89	14.20	12.12	10.52	10.08	9.45	9.21	5.57	4.97	3.40
3 bits	RTN	1284.92	64.57	119.47	298.00	23.54	46.04	18.80	6122.33	6.66	5.52	3.98
	GPTQ [8]	53.43	32.28	20.90	16.55	12.88	11.58	10.29	9.90	6.43	5.48	3.88
	OWQ [9] (3.01 bits)	35.26	26.59	16.40	13.21	11.21	11.48	9.59	9.28	6.21	5.36	3.77
	AWQ [10]	36.77	–	16.32	13.54	11.41	10.67	9.85	9.63	6.24	5.32	3.74
	CVXQ (Ours)	30.71	25.96	14.75	12.42	11.07	10.28	9.56	9.29	6.00	5.25	3.76

Table 2: Effect of hyperparameters on quantized model accuracy. Quantized model accuracy is relatively insensitive to the batch size (a) and number of tokens per sequence (b) used for optimization. Smaller clusters improve quantized model accuracy at lower average bit depths (c). Perplexity measured on the C4 test set.

(a) Minibatch size and PPL					(b) Number of tokens and PPL					(c) Cluster size and PPL							
C4 (↓)	OPT (4 bits)		OPT (3 bits)		C4 (↓)	OPT (4 bits)		OPT (3 bits)		C4 (↓)	OPT (4 bits)		OPT (3 bits)				
	1.3B	13B	1.3B	13B		1.3B	13B	1.3B	13B		1.3B	13B	1.3B	13B			
FP16	16.07	12.06	16.07	12.06	FP16	16.07	12.06	16.07	12.06	FP16	16.07	12.06	16.07	12.06			
Batch size	2	16.24	12.12	16.94	12.36	Num tokens	3	16.40	12.29	17.05	12.47	Cluster size	64	16.16	12.10	16.62	12.26
	4	16.24	12.12	16.94	12.35		5	16.28	12.18	16.93	12.37		128	16.17	12.10	16.70	12.29
	8	16.25	12.11	16.90	12.34		9	16.24	12.12	16.91	12.35		256	16.20	12.10	16.77	12.32
	16	16.22	12.11	16.86	12.32		17	16.22	12.11	16.86	12.32		512	16.22	12.11	16.86	12.32
	32	16.24	12.12	16.88	12.36		33	16.21	12.10	16.87	12.34		1024	16.23	12.11	16.99	12.42

Table 3: Pruning and overhead bits due to quantization. A small fraction of weights are quantized to zero and pruned away due to low variance, with smaller clusters increasing the degree of pruning (a). Quantization incurs overhead bits for signaling cluster indices and location and scale parameters of each weight cluster (b).

(a) Pruned columns (%) in quantized models								(b) Overhead bits (%) from quantization parameters								
Pruned (%)	OPT (4 bits)			OPT (3 bits)			Overhead bits (%)	OPT (4 bits)			OPT (3 bits)			30B		
	350M	1.3B	13B	350M	1.3B	13B		350M	1.3B	13B	350M	1.3B	13B			
Cluster size	64	0.57	2.13	2.18	0.64	3.70	3.12	Cluster size	64	10.33	10.30	10.28	13.77	13.73	13.71	13.70
	128	0.61	2.19	2.31	0.68	3.81	3.04		128	5.18	5.16	5.15	6.91	6.88	6.87	6.86
	256	0.67	2.10	2.16	0.69	3.06	2.69		256	2.60	2.59	2.58	3.47	3.45	3.44	3.44
	512	0.68	2.07	2.00	0.70	2.85	2.57		512	1.30	1.30	1.30	1.73	1.73	1.73	1.72
	1024	0.68	2.08	1.92	0.70	2.39	2.26		1024	0.64	0.65	0.65	0.85	0.87	0.87	0.86

Table 4: Grade School Math 8K (GSM8K) and 2.x-bit quantization. Quantized model accuracy translates to performance on tasks such as GSM8K (cluster size of 256 is used) (a). Quantized to 2.x bits per weight on average, CVXQ provides a significant perplexity reduction compared to OWQ models quantized to the same.

(a) Percentage score of correct answers on GSM8K							(b) Perplexity of 2.1–2.8 bit-quantized models					
Score (%)	Llama 2 (4 bits)			Llama 2 (3 bits)			Perplexity	Llama 2 7B (2.1–2.8 bits)				
	7B	13B	70B	7B	13B	70B		WikiText2 (↓)	2.1	2.2	2.4	2.6
FP16	14.10	23.43	53.90	14.10	23.43	53.90	FP16	5.47	5.47	5.47	5.47	5.47
RTN	7.05	19.11	46.93	1.82	1.67	6.14	OWQ [9]	39.56	11.25	10.79	10.43	10.24
GPTQ/256	11.60	21.46	52.01	6.60	14.48	46.47	OWQ/256	10.34	10.01	9.98	9.50	9.26
AWQ/256	14.33	23.12	50.34	6.97	16.76	48.07	OWQ/128	10.01	9.66	9.42	9.38	9.14
CVXQ/256	12.74	23.05	53.37	8.87	18.04	48.60	CVXQ/256	9.47	8.39	7.05	6.56	6.21

more accurate at these bit depths than their OWQ counterparts. This is expected since CVXQ assigns bit depths from the range $(0, B_{\max})$ commensurately with gradient variances whereas OWQ simply preserves a fixed number of high-variance weights in 16 bits (FP16) and quantizes the rest to 2 bits.

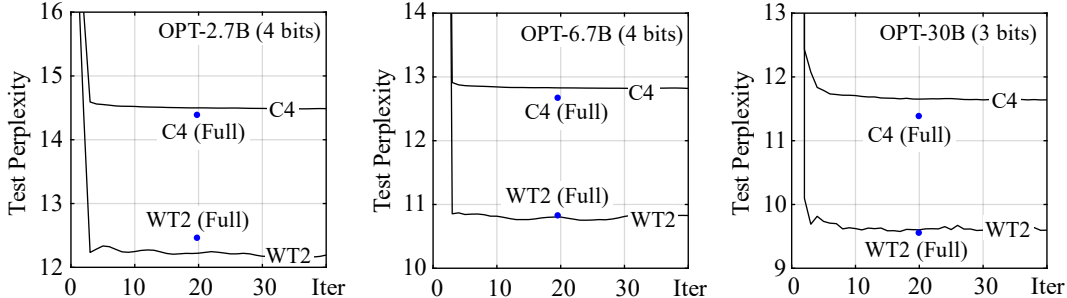


Figure 5: Test perplexity across iterations. Calibrated on C4 (train) using a minibatch size of 16. Row clusters used with a cluster size of 512. Perplexity decreases rapidly within the first 30 iterations, monotonically for C4 (test), whose distribution is similar to the calibration data, and with some oscillations for WikiText2 (test).

5 DISCUSSION

Formulating weight quantization as a convex optimization problem, as we have done here, bestows several benefits. First, it explicates the objective we seek to optimize (minimizing output distortion in our case) and sets us on a path to solve the right problem using modern automatic differentiation tools e.g. PyTorch’s autograd package. Second, our formulation enables us to interpret many of the previous Hessian-based approaches [8–11] as heuristics for approximate optimization of the true underlying objective. Note that (2) is a nonlinear system of equations in bit depth variables, so any non-iterative solution is necessarily only an approximate one if one’s goal is to optimize an objective similar to (2). It is interesting to see that recent high-performing model quantization methods [7–9] can ultimately trace their lineage back to the classic Optimal Brain Surgeon [31] algorithm, which is a convex formulation for weight pruning as opposed to quantization.

Our experimental results indicate that an accurate characterization of the quantization problem can indeed lead to better compression outcomes. While the smaller OPT-125M model is too limited for practical use in many situations, its relative incompressibility helps contrast the performance of the different weight quantization methods themselves (Table 1). With larger models like OPT-66B and Llama 2-66B, most approaches (including RTN) perform similarly, suggesting that larger language models are more compressible in general. At first glance, RTN may seem sufficient for quantizing larger models. However, RTN-quantized models lead to severely reduced accuracy on downstream tasks such as GSM8K (Table 4 (a)), which highlights the importance of validating the accuracy of quantized models across multiple tasks and datasets.

Limitations and future work. In a sense, the end-to-end nature of our optimization algorithm can also be its own weakness, as convergence can be slower for low-bit (2 bit) instances of problem (3) and the algorithm can require more hardware resources than previous methods. Extensions currently underway for weight quantization include faster optimizers and optimal compander design. Unlike GPTQ and its extensions, the proposed method spends most of its running time on the collection of channel statistics (squares of gradients) and very little time on the actual quantization process. This allows us to apply CVXQ also to activation quantization, in which quantization efficiency becomes paramount. We discuss activation quantization and other CUDA implementation-specific details in our sequel—Part 2: Activation Quantization.

ACKNOWLEDGMENTS

If you have found this work useful, please consider gifting computational resources to support our ongoing research efforts. The author expresses his sincere gratitude for the compute cluster kindly made available for use by the Massachusetts Life Sciences Center (MLSC).

REFERENCES

- [1] Markus Nagel, Rana Ali Amjad, Mart Van Baalen, Christos Louizos, and Tijmen Blankevoort. Up or down? Adaptive rounding for post-training quantization. In *Proc. ICML*, 2020.

- [2] Itay Hubara, Yury Nahshan, Yair Hanani, Ron Banner, and Daniel Soudry. Accurate post training quantization with small calibration sets. In *Proc. ICML*, 2021.
- [3] Yuhang Li, Ruihao Gong, Xu Tan et al. BRECCQ: Pushing the limit of post-training quantization by block reconstruction, In *Proc. ICLR*, 2021.
- [4] Tim Dettmers, Mike Lewis, Younes Belkada, and Luke Zettlemoyer. GPT3.int8(): 8-bit matrix multiplication for transformers at scale. In *Proc. NeurIPS*, 2022.
- [5] Zhewei Yao, Reza Yazdani Aminabadi, Minjia Zhang, Xiaoxia Wu, Conglong Li, and Yuxiong He. ZeroQuant: Efficient and affordable post-training quantization for large-scale transformers. In *Proc. NeurIPS*, 2022.
- [6] Guangxuan Xiao, Ji Lin, Mickael Seznec, Hao Wu, Julien Demouth, and Song Han. SmoothQuant: Accurate and efficient post-training quantization for large language models. In *Proc. ICML*, 2023.
- [7] Elias Frantar, and Dan Alistarh. Optimal Brain Compression: A framework for accurate post-training quantization and pruning. In *Proc. NeurIPS*, 2022.
- [8] Elias Frantar, Saleh Ashkboos, Torsten Hoefler, and Dan Alistarh. OPTQ: Accurate quantization for generative pre-trained transformers. In *Proc. ICLR*, 2022.
- [9] Changhun Lee, Jungyu Jin, Taesu Kim, Hyungjun Kim, and Eunhyeok Park. OWQ: Outlier-aware weight quantization for efficient fine-tuning and inference of large language models. In *Proc. AAAI*, 2024.
- [10] Zhen Dong, Zhewei Yao, Amir Gholami, Michael W. Mahoney, and Kurt Keutzer. HAWQ: Hessian AWARE Quantization of neural networks with mixed-precision. In *Proc. ICCV*, 2019.
- [11] Weihang Chen, Peisong Wang, and Jian Cheng. Towards mixed-precision quantization of neural networks via constrained optimization. In *Proc ICCV*, 2021.
- [12] Ji Lin, Jiaming Tang, Haotian Tang et al. AWQ: Activation-aware Weight Quantization for on-device LLM compression and acceleration. In *Proc. MLSys*, 2024.
- [13] Schoon Kim et al. SqueezeLLM: Dense-and-sparse quantization. In *Proc. ICML*, 2024.
- [14] Wenqi Shao et al. OmniQuant: Omnidirectionally calibrated quantization for large language models. In *Proc. ICLR*, 2024.
- [15] Tim Dettmers et al. SpQR: A Sparse-Quantized Representation for near-lossless LLM weight compression. <http://arxiv.org/abs/2306.03078>, 2023.
- [16] Vincent Vanhoucke, Andrew Senior, and Mark Z. Mao. Improving the speed of neural networks on CPUs. In *Proc. NIPS Workshops*, 2011.
- [17] Aojun Zhou, Anbang Yao, Yiwen Guo, Lin Xu, and Yurong Chen. Incremental Network Quantization: towards lossless CNNs with low-precision weights. In *Proc. ICLR*, 2017.
- [18] Benoit Jacob et al. Quantization and training of neural networks for efficient integer-arithmetic-only inference. In *Proc. CVPR*, 2018.
- [19] Dongqing Zhang, Jiaolong Yang, Dongqiangzi Ye, and Gang Hua. LQ-Nets: Learned Quantization for highly accurate and compact deep neural networks. In *Proc. ECCV*, 2018.
- [20] Steven K. Esser, Jeffrey L. McKinstry, Deepika Bablani, Rathinakumar Appuswamy, and Dharmendra S. Modha. Learned step size quantization. In *Proc. ICLR*, 2019.
- [21] Yoojin Choi, Mostafa El-Khamy, and Jungwon Lee. Towards the limits of network quantization. In *Proc. ICLR*, 2017.
- [22] Kuan Wang, Zhijian Liu, Yujun Lin, Ji Lin, and Song Han. HAQ: Hardware-aware automated quantization with mixed precision. In *Proc. CVPR*, 2019.
- [23] Ritchie Zhao, Yuwei Hu, Jordan Dotzel, Chris De Sa, and Zhiru Zhang. Improving neural network quantization without retraining using outlier channel splitting. In *Proc. ICML*, 2019.
- [24] Lu Hou, and James T. Kwok. Loss-aware weight quantization of deep networks. In *Proc. ICLR*,

2018.

- [25] Yury Nahshan, Brian Chmiel, Chaim Baskin, Evgenii Zheltonozhskii, Ron Banner, Alex M. Bronstein, and Avi Mendelson. Loss aware post-training quantization. In *Mach Learn* 110 3245–3262, Springer, 2020.
- [26] Zhongnan Qu, Zimu Zhou, Yun Cheng, and Lothar Thiele. Adaptive loss-aware quantization for multi-bit networks. In *Proc. CVPR*, 2020.
- [27] Markus Nagel, Mart van Baalen, Tijmen Blankevoort, and Max Welling. Data-free quantization through weight equalization and bias correction. In *Proc. CVPR*, 2019.
- [28] Shoukai Xu, Haokun Li, Bohan Zhuang, Jing Liu, Jiezhong Cao, Chuangrun Liang, and Mingkui Tan. Generative low-bitwidth data free quantization. In *Proc. ECCV*, 2020.
- [29] Kanghyun Choi, Deokki Hong, Noseong Park, Youngsok Kim, and Jinho Lee. Qimera: Data-free quantization with synthetic boundary supporting samples. In *Proc. NeurIPS*, 2021.
- [30] Biao Qian, Yang Wang, Richang Hong, and Meng Wang. Adaptive data-free quantization. In *Proc. CVPR*, 2023.
- [31] Babak Hassibi, and David Stork. Second order derivatives for network pruning: Optimal Brain Surgeon. In *Proc. NIPS*, 1992.
- [32] Yunchao Gong, Liu Liu, Ming Yang, and Lubomir Bourdev. Compressing deep convolutional networks using vector quantization. In *ICLR* 2015.
- [33] Allen Gersho, and Robert M. Gray. Vector Quantization and Signal Compression. Kluwer, Norwell, MA, USA 1991.
- [34] Stephen Boyd, Neal Parikh, Eric Chu, Borja Peleato, and Jonathan Eckstein. Distributed Optimization and Statistical Learning via the Alternating Direction Method of Multipliers. *Found. Trends® Mach. Learn.*, 3(1):1–122, 2011.
- [35] Thomas M. Cover, and Joy A. Thomas. Elements of Information Theory (Wiley Series in Telecommunications and Signal Processing). Wiley-Interscience, USA 2006.
- [36] S. Lloyd. Least squares quantization in PCM. *IEEE Trans. Inf. Theory*, 28(2):129–137, 1982.
- [37] J. Max. Quantizing for minimum distortion. *IRE Trans. Inf. Theory*, 6(1):7–12, 1960.
- [38] R.M. Gray, and D.L. Neuhoff. Quantization. *IEEE Trans. Inf. Theory*, 44(6):2325–2383, 1998.
- [39] Susan Zhang, Stephen Roller, Naman Goyal et al. OPT: Open Pre-trained Transformer Language Models. <http://arxiv.org/abs/2205.01068>, 2022.
- [40] Hugo Touvron, Louis Martin, Kevin Stone et al. Llama 2: Open foundation and fine-tuned chat models. <http://arxiv.org/abs/2307.09288>, 2023.
- [41] Colin Raffel, Noam Shazeer, Adam Roberts et al. Exploring the limits of transfer learning with a unified text-to-text transformer. *J. Mach. Learn. Res.*, 21(140):1–67, 2020.
- [42] Stephen Merity, Caiming Xiong, James Bradbury, and Richard Socher. Pointer sentinel mixture models. In *Proc. ICLR*, 2022.
- [43] Karl Cobbe, Vineet Kosaraju, Mohammad Bavarian et al. Training verifiers to solve math word problems. <http://arxiv.org/abs/2110.14168>, 2021.